EPJ Web of Conferences **94**, 01022 (2015)
DOI: 10.1051/epjconf/20159401022

Influence of the temperature on the tension behaviour of EUROFER97 alloy at high strain rate

Ezio Cadoni[1,a], Matteo Dotta[1], Daniele Forni[1,2], and Philippe Spätig[3]

[1]DynaMat Laboratory, University of Applied Sciences of Southern Switzerland, 6952 Canobbio, Switzerland
[2]Department of Structural, Geotechnical and Building Engineering - Politecnico di Torino, 10129 Torino, Italy
[3]Laboratory for Nuclear Materials, Nuclear Energy and Safety Research Department,Paul Scherrer Institut, 5232 Villigen PSI, Switzerland

Abstract. This paper presents an experimental investigation on the influence of the temperature on the reduced activation steel Eurofer97 under uniaxial tensile loads at high strain rate. Round undamaged specimens of this material having gauge length 5 mm, diameter 3 mm, were tested in universal machine to obtain its stress-strain relation under quasi-static condition ($0.001 s^{-1}$), and in modified Hopkinson bar to study its mechanical behaviour at high strain rates ($300\,s^{-1}$, $1000\,s^{-1}$) respectively. The tests at high strain rate were carried out at 450 °C and at nitrogen temperature. Finally, the parameters of the Zerilli-Armstrong constitutive material relationship were obtained.

1. Introduction

In a real fusion reactor, plasma disruptions are expected to occur that will yield disruption stress peaking in about 1 ms: that represents the typical loading rate of dynamical tests. Thus, up to now, not enough attention has been paid to characterize both the dynamic constitutive behaviour and dynamic fracture toughness behaviour of the tempered martensitic steels. As a first step to fill that gap, this study has been undertaken to investigate the tensile properties, yield stress and strain hardening, from static to highly dynamic regime of Eurofer97 steel. Those data are necessary to calculate the stress/strain field around the crack tip by finite element simulations to model the toughness-temperature behaviour in the transition region This paper presents an experimental investigation on the influence of the temperature of reduced activation steel Eurofer97 under uniaxial tensile loads at high strain rate. Round undamaged specimens of this material having gauge length 5 mm, diameter 3 mm, were tested in universal machine to obtain its stress-strain relation under quasi-static condition ($0.001\,s^{-1}$), and in modified Hopkinson bar to study its mechanical behaviour at high strain rates ($300\,s^{-1}$, $1000\,s^{-1}$) respectively. The test at high strain rate were carried out at 450 °C and at nitrogen temperature.

2. Material

The reduced activation steel Eurofer97 is a tempered-martensitic stainless steel of the 7–9wt% Cr class. The concentration of the main alloying elements is (in wt%) 0.1% C, 8.9% Cr, 1% W, 0.2% V and 0.15% Ta. In order to obtain the reduced-activation behaviour, several alloying elements commonly added to commercial martensitic stainless steels like Ni, Nb and Mo have been either removed (Ni), or replaced (Nb and Mo) by elements with shorter half lives (W, V, Ta). Eurofer97 has been selected by EU as reference structural material and will be used to fabricate the Test Blanket Modules of the International Thermonuclear Fusion Reactor (ITER) [1]. The material has been produced by Bölher AG as rolled plates of 8, 14 and 25 mm. In this work, we have studied the material coming from the 25 mm plate of the heat 9741. The final thermal treatment applied consisted of austenitization during 0.5h @ 980 °C + air cooling followed by tempering 1.5 h @ 760 °C + air cooling. A detailed description of the microstructure of the Eurofer97 can be found in [2] and [3]. Here, it suffices to say that the material features small prior austenitic grains, characterized by a mean intercept length of about 10 μm. The carbides, mainly M_23C_6 and TaC type, are not bigger than 400 μm. This steel is very clean and its inclusions level is extremely low.

3. Experimental set-up

The high strain rate tests were carried out by means of a Split Hopkinson Tensile Bar (SHTB) device shown in Fig. 1. It consists of two cylindrical high strength steel bars, having a diameter of 10 mm, with a length of 9 and 6 m for input and output bar, respectively and the thin sheet steel specimen is screwed to the two bars [4–8].

The test with the SHTB is performed as follows: 1) first a hydraulic actuator, of maximum loading capacity of 600 kN, is pulling part of the input bar (6 m) as pretension bar with a diameter of 10 mm; the pretension stored in this bar is resisted by the blocking device; 2) second operation is the rupture of the brittle bolt in the blocking device which gives rise to a tensile mechanical pulse of 2.4 ms duration with linear loading rate during the rise

[a] Corresponding author: ezio.cadoni@supsi.ch

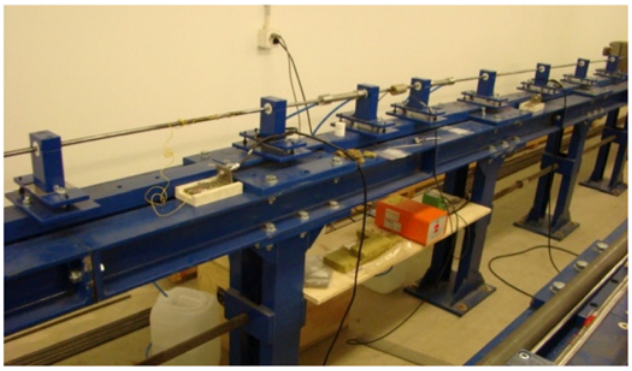

Figure 1. SHTB device.

time (30 μs), propagating along the input and output bars bringing to fracture the specimen.

The input and output bars are instrumented with strain gauges, which measure the incident, reflected and transmitted pulses acting on the cross section of the specimen. As pre-tensioned bar is used part of the input bar. On the basis of the incident (ε_I), reflected (ε_R) and transmitted (ε_T) records, of the consideration of the basic constitutive equation of the input and output elastic bar material, of the one-dimensional wave propagation theory it is possible to calculate the stress, strain and strain-rate curves by the following equations [4–8]:

$$\sigma_E(t) = E_0 \frac{A_0}{A} \varepsilon_T(t) \tag{1}$$

$$\varepsilon_E(t) = -\frac{2C_0}{L} \int_0^t \varepsilon_R(t)\, dt \tag{2}$$

$$\dot{\varepsilon}(t) = -\frac{2C_0}{L} \varepsilon_R(t) \tag{3}$$

where: E_0 is the elastic modulus of the bars; A_0 their cross-sectional area; A is the specimen cross section area; L is the specimen gauge length; C_0 is the sound velocity of the bar material.

In order to test the EUROFER97 steel at high temperature and high strain rate a homemade oven was used. In Fig. 2 the high temperature set-up is shown. It consists of an oven, able to maintain constant the temperature (measured by a thermocouple in contact with the specimen), and cooling systems to avoid any influence on the strain gauges.

The low temperature tests were obtained by means of a system containing nitrogen liquid as shown in Fig. 3. The test starts when the temperature of the specimen is in equilibrium with the nitrogen liquid.

4. Results

The results of the experiments carried out at room temperature (293°K) are summarized in Table 1 [6]. It can be noted as the flow stress increases with increasing strain rate, at room temperature.

The high strain rate results at high and low temperature are shown in Table 2 and Table 3, respectively.

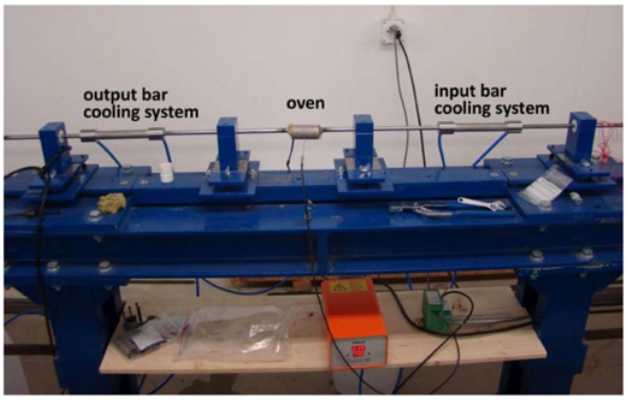

Figure 2. Set-up for high temperature high strain rate testing.

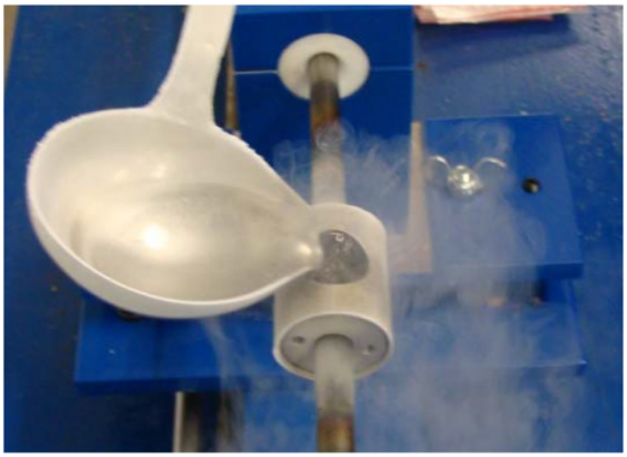

Figure 3. Experimental set-up for low temperature testing.

Table 1. Strain rate results at room temperature [6].

Strain-rate [s^{-1}]	$R_{0.2}$ [MPa]	R_m [MPa]	Uniform strain [%]	Reduction of area Z [%]
10^{-3}	560	652	4.8	80.7
5	665	753	8.6	77.2
30	680	783	6.4	78.1
300	716	814	10.0	77.7
600	720	837	11.5	77.3

It can be observed as the strength decrease increasing the test temperature. The reduction of area increase with increasing strain rate and temperature as also shown in Fig. 4, where the stress versus strain curves at high strain rate and different temperature are depicted.

The true stress and true strain were obtained by:

$$\sigma_{true} = \sigma_{eng}\left(1 + \varepsilon_{eng}\right) \tag{4}$$

$$\varepsilon_{true} = \ln\left(1 + \varepsilon_{eng}\right). \tag{5}$$

The true stress vs. strain curves must be regarded as significant until the point of ultimate tensile stress where the necking begins; after this point localization and fracture propagation governs the flow curve, which

Table 2. Strain rate results @723K.

Strain-rate [s^{-1}]	$R_{0.2}$ [MPa]	R_m [MPa]	Uniform strain [%]	Reduction of area Z [%]
568	321	473	5.07	86.53
548	383	517	5.57	86.28
1318	463	496	2.31	88.32
1955	404	412	4.00	89.66

Table 3. Strain rate results @77K.

Strain-rate [s^{-1}]	$R_{0.2}$ [MPa]	R_m [MPa]	Uniform strain [%]	Reduction of area Z [%]
228	1364		0.77	2.0
246	1203		0.65	0.0
982	858		0.39	0.0
1000	1288		0.61	0.0

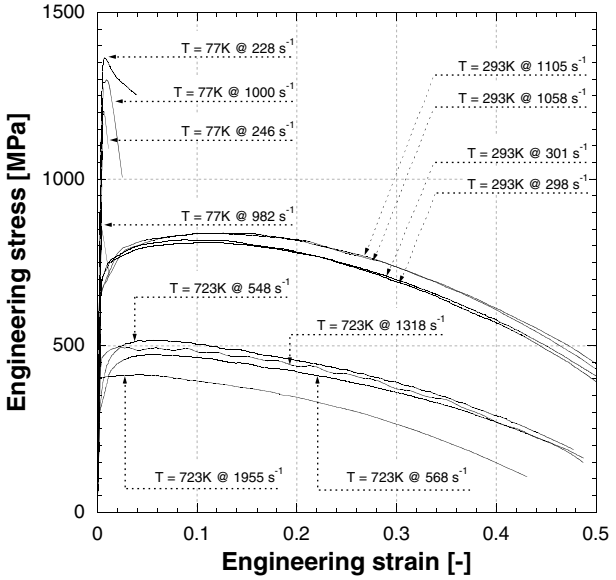

Figure 4. Stress vs. strain curves at high strain rate and different temperature.

is no more representative of homogeneous mechanical properties of the materials. In this case beyond the point of uniform straining of the engineering stress-strain curve the one-dimensional true stress-strain curve should be reconstructed by calculating the true stress and the true strain using the Bridgman formulae [9] which introduce the correction for the tri-axial stress state. At fracture the Bridgman formulae can be written as follows:

$$\sigma_{\text{true,fracture}} = \frac{\sigma_{\text{eng.,fracture}}}{(1 + 2R/a) \cdot \ln(1 + a/2R)} \tag{6}$$

where, a is minimum radius at fracture cross-section, R is the meridional profile radius at fracture neck (see Figs. 5–6), and $\sigma_{\text{true,fracture}} = P_{\text{fracture}}/\pi a^2 g$ the average stress at fracture and P_{fracture} the fracture force.

$$\varepsilon_{\text{true,fracture}} = 2 \cdot \ln \frac{a_0}{2 \cdot a} \tag{7}$$

where, a_0 is the initial diameter of the gauge length cross-section.

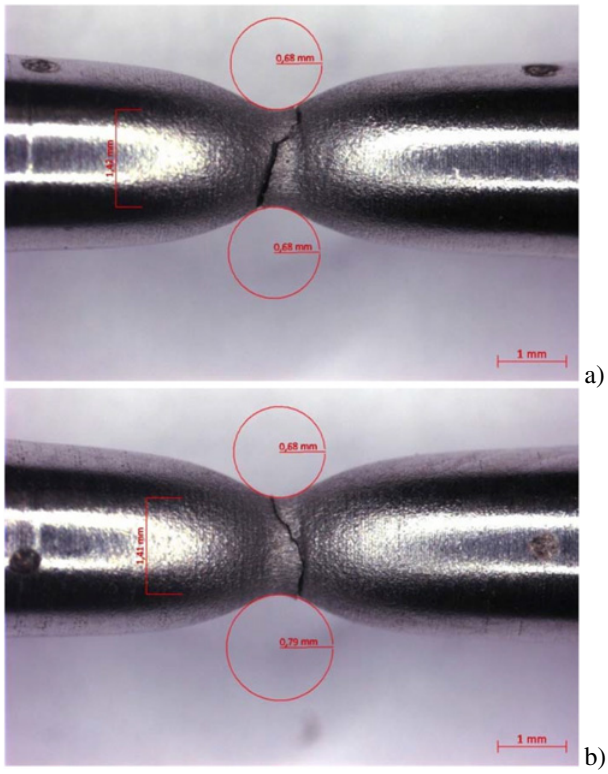

Figure 5. Dynamic test at 293K @: a) 1000 s^{-1} and b) 300 s^{-1}.

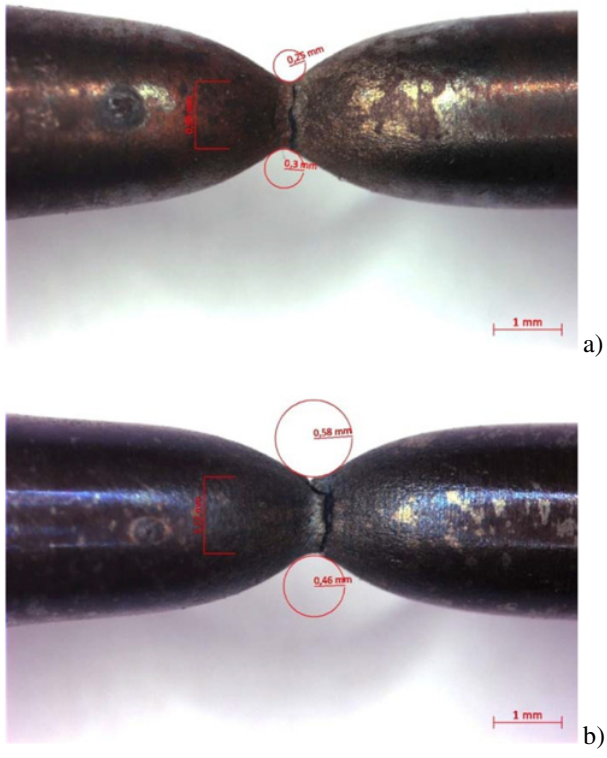

Figure 6. Dynamic test at 723K @: a) 1000 s^{-1} and b) 600 s^{-1}.

Having calculated the true stress and true strain at fracture with the Eqs. (4) and (5) for the complete construction of the true stress-strain curve during the necking deformation phase a straight line is drawn between

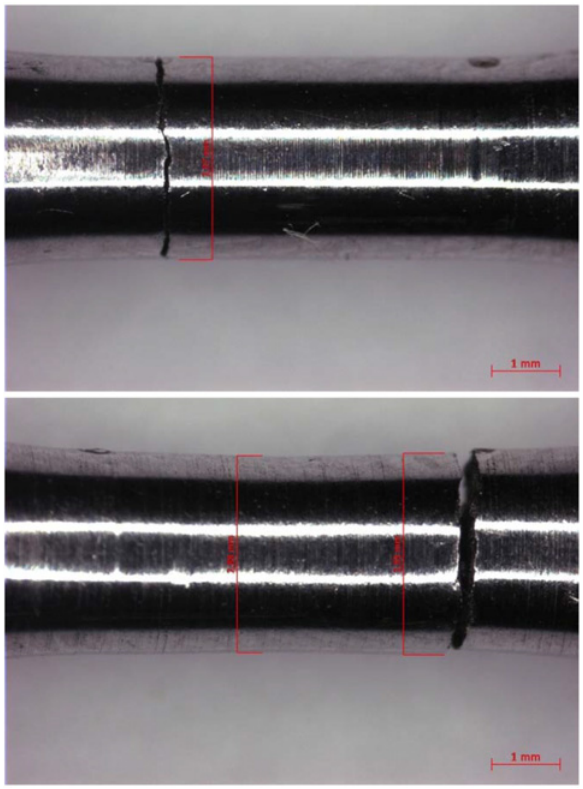

Figure 7. Dynamic test at 77K @: a) 1000 s^{-1} and b) 300 s^{-1}.

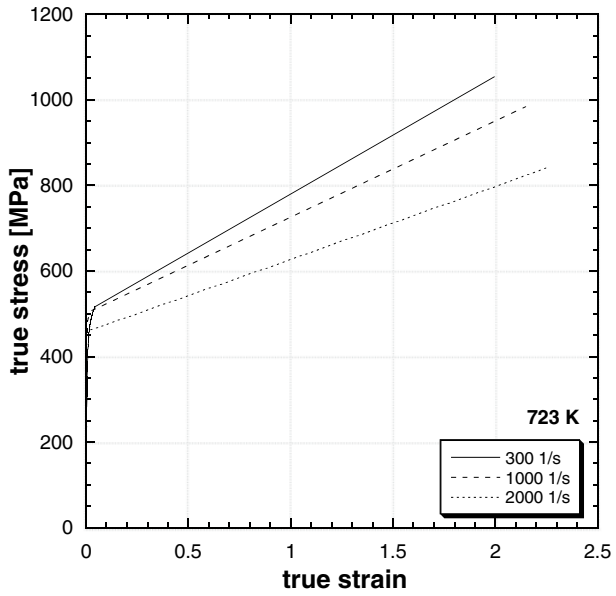

Figure 8. True stress vs. true strain curves @723K and different high strain rates.

the ultimate tensile strength/uniform strain point and the fracture point determined by application of the Eqs. (6) and (7).

In Fig. 8 the true stress versus true strain of the test at high strain rate and high temperature are shown. It can be noted as the strain hardening decreases with increasing the strain rate.

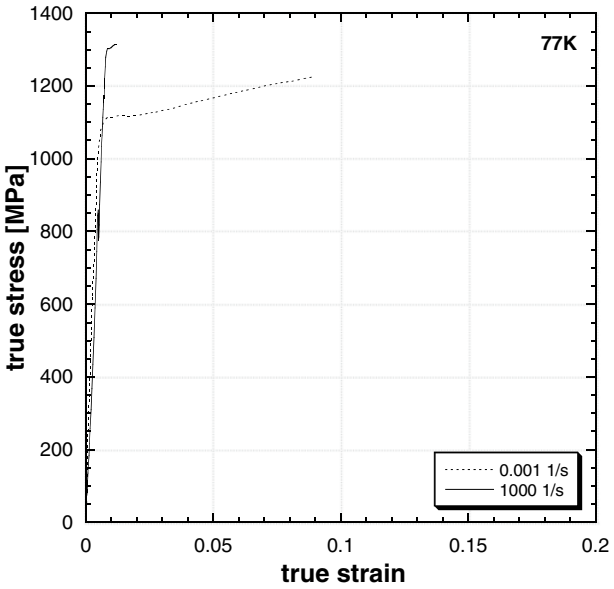

Figure 9. Comparison between quasi-static and dynamic true stress vs. true strain curves @77K.

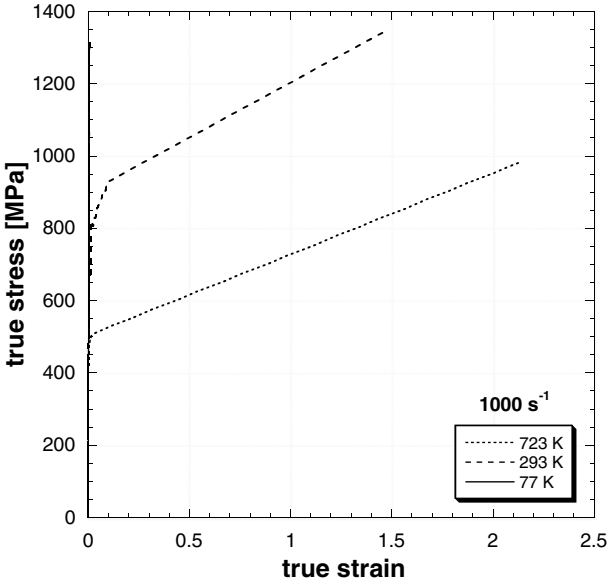

Figure 10. True stress vs. true strain curves @1000 s^{-1} and different temperatures.

Figure 9 shows the comparison between quasi-static and dynamic true stress versus strain curves at low temperature. The failure at high strain rate could be influenced by the presence of marks (see Fig. 7) produced manually by means of an electrical pencil device. At this temperature all failure start in correspondence of such surface discontinuity, and this could be the reason causing the premature failure of the test at 982 s^{-1}.

Comparing the true stress versus true strain curves (see Fig. 10) at the same strain rate but at different temperature is possible to observe the influence of the temperature. The brittleness of the material increases with the decrease of the temperature.

The influence of the temperature can be better understood analysing the yield stress in function of the

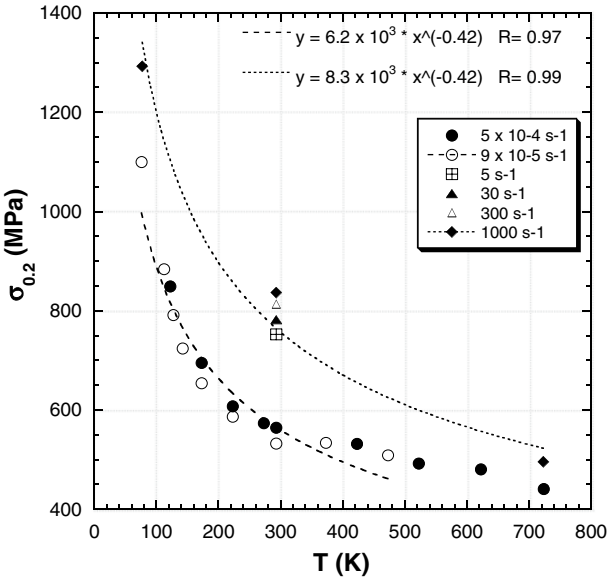

Figure 11. Yield stress vs. temperature for different strain rates.

temperature as illustrated in Fig. 11. Indeed, adding the results obtained at high strain rate to those obtained in quasi-static regime [2] at $9{\cdot}10^{-5}\mathrm{s}^{-1}$ can be highlighted how the strain rate vertically moves the curve. The behaviour is well described by an exponential function.

5. Constitutive model

It is commonly known that many constitutive relations are simply a numerical fit to test data. At best these models include work hardening, strain-rate dependence as well as the thermal softening such as the well-known model proposed by Johnson and Cook in the eighties [10] and nowadays widely used. On the other hand, there are other models based upon physical concept such as Zerilli-Armstrong material constitutive model [11], based upon dislocation mechanics. Others authors based their constitutive model upon dislocation density [2,3,6].

To describe the influence of temperature effect on the dynamic behaviour of Eurofer97, that is a body centered metal [1], the Zerilli-Armstrong was used. The relationship proposed for bcc metals is:

$$\sigma = c_0 + c_1 \cdot \exp\left(-c_3 \cdot T + c_4 \cdot T \cdot ln(\dot{\epsilon})\right) + c_5 \epsilon^n \quad (8)$$

where, c_1, c_3, c_4, c_5 and n are the five material constants for the bcc model, while c_0 take into account the influence of the dislocation density on the yield stress [2], evaluable as follow:

$$c_0 = \Delta_{\sigma'_G} + k \cdot l^{-1/2}. \quad (9)$$

This last parameter was chosen equal to 55 MPa thanks to a previous investigation of the plastic flow properties in tension of the Eurofer97 steel [2]. As a first approximation, the obtained five material constants are collected in the following Table 1.

In order to check the validity of the obtained constants, a comparison between experimental and Zerilli-Armstrong fit has been depicted in Fig. 12. Three

Table 4. Zerilli-Armstrong parameter for the Eurofer97.

c_1 [MPa]	c_3 [$^\circ\mathrm{K}^{-1}$]	c_4 [$^\circ\mathrm{K}^{-1}$]	c_5 [MPa]	n [-]
1075	$2{,}063 \cdot 10^{-3}$	$6{,}762 \cdot 10^{-5}$	673,1	0,5320

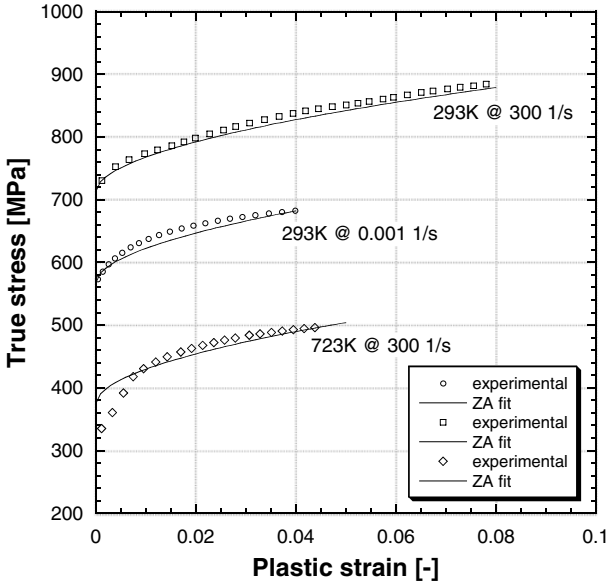

Figure 12. Comparison between Zerilli-Armstrong fits and experimental data.

different experimental tests and the constitutive model were compared: quasi-static at room temperature (293 K), high-strain-rate at room (293 K) and high temperature (723 K).

6. Conclusions

The effect of high and low temperature at high strain rates on the tensile properties of the tempered martensitic steel Eurofer97 was studied by means of a Split Hopkinson Tensile Bar device.

This tempered-martensitic stainless steel showed a quite high strain rate sensitivity. Furthermore, it shows a moderately high sensitivity to temperature at high strain rate.

Finally, the material parameters of the Zerilli-Armstrong constitutive equation were determined. The use of this calibration seems to fit relatively well with the experimental data.

References

[1] Standard Test Method for Determination of Reference Temperature, T_0, for Ferritic Steels in the Transition Range, E1921-08, Annual Book of ASTM Standards 2008, vol. 03.01, ASTM International, 2008.

[2] P. Spätig, R. Bonadé, G. R. Odette, J. W. Rensman, N. Campitelli, P. Mueller, J. Nucl. Mat. **367–370**, 527–538 (2007).

[3] E. Lucon, R. Chaouadi, M. Decréton, J. Nucl. Mater. **329–333** 1078 (2004).

[4] E. Cadoni, L. Fenu, D. Forni, Constr. Build. Mat. **35**, 399–407 (2012).
[5] D. Asprone, E. Cadoni, A. Prota, ACI Struct. J. **106**, 523–529 (2009).
[6] E. Cadoni, M. Dotta, D. Forni, P. Spätig, J. Nucl. Mat. **414**(3), 360–366 (2011)
[7] E. Cadoni, M. Dotta, D. Forni, N. Tesio, C. Albertini, Mat. Des. **49**, 657–666 (2013).
[8] C. Albertini, E. Cadoni, G. Solomos, *Phil. Trans. Roy. Soc. A:* **372**, 20130197, (2014).
[9] Bridgman PW (1952) *Studies in large plastic flow and fracture.* McGraw-Hill, New York
[10] G.R. Johnson, W.H. Cook, *Eng. Fract. Mech.* **21**, 31 (1985)
[11] F.J. Zerilli, R.W. Armstrong, *J. Appl. Phys.* **61**(5), (1987)